

## Cotidal Charts near Hawaii Derived from TOPEX/Poseidon Altimetry Data

LI-LI FAN, BIN WANG, AND XIAN-QING LV

*Physical Oceanography Laboratory, Ocean University of China, Qingdao, Shandong, China*

(Manuscript received 1 July 2010, in final form 17 October 2010)

### ABSTRACT

Harmonic analysis of 10 yr of Ocean Topography Experiment (TOPEX)/Poseidon (T/P) along-track altimetry is performed to derive the semidiurnal and diurnal tides ( $M_2$ ,  $S_2$ ,  $N_2$ ,  $K_2$ ,  $K_1$ ,  $O_1$ ,  $P_1$ , and  $Q_1$ ) near Hawaii. The T/P solutions are evaluated through intercomparison for crossover points of the ascending and descending tracks and comparison with the data of tidal stations, which show that the T/P solutions in the study area are reliable. By using a suitable order polynomial to fit the T/P solutions along every track, the harmonic constants of any point on T/P tracks are acquired. A new fitting method, which is characterized by applying the harmonics from T/P tracks to produce directly empirical cotidal charts, is developed. The harmonic constants derived by this fitting method show good agreement with the data of tidal stations, the results of National Astronomical Observatory 99b (NAO.99b), TOPEX/Poseidon 7.2 (TPXO7.2), and Finite Element Solutions 2004 (FES2004) models, which suggests that the fitting method is reasonable, and the highly accurate cotidal chart could be directly acquired from T/P altimetry data by this fitting method.

### 1. Introduction

The studies of tides and cotidal charts have a long history. At the early stage, the cotidal charts of certain sea areas mainly depended on observations at coastal and island tidal gauge stations (e.g., Ogura 1933; Nishida 1980; Fang 1986), but the information of tides obtained by these direct observation methods is very limited. Since the launch of satellite altimetry Ocean Topography Experiment (TOPEX)/Poseidon (T/P) in August 1992, which provides unprecedented precise sea surface height data, the study of ocean tides has progressed dramatically. Especially in the past 10 yr, T/P altimeter data have been widely used to study the distribution and characteristics of ocean tides and build either a global or regional tidal model. The first application of T/P altimeter data covering about 7 months was carried out to derive ocean tides in the Asian semi-enclosed sea by Mazzega and Berge (1994). By interpolating the tidal variations of the sea surface, Yanagi et al. (1997) used T/P altimeter data covering about 3 yr to construct cotidal charts of eight tidal constituents in the Yellow and East China Seas, showing significant improvement over Mazzega and

Berge's work. Teague et al. (2000) evaluated the tides in the Bohai and Yellow Seas derived from 5 yr of T/P data through a comparison with data from in situ pressure gauges and coastal tide stations, and their fairly good agreement suggested that T/P could provide accurate tide data in specific regions. Fang et al. (2004) applied the tidal harmonics from T/P altimetry data covering 10 yr at coastal and island stations to give empirical cotidal charts of five principal constituents in the Bohai, Yellow, and East China Seas, showing higher accuracy than the previous charts for the offshore area. They acquired the harmonics at every grid point by using quadratic polynomials to fit its surrounding data points within a certain influence distance in the T/P track coordinates. In short, the new methods have been emerging in an endless stream and the study of ocean tides has also significantly improved with the satellite altimeter data increasing.

In this paper, we propose a new fitting method that is quite different from other existing methods and models. It does not depend on the complex dynamic system and has nothing to do with models, so that terrible calculations are avoided. The method is characterized by applying the harmonics from T/P tracks to produce directly empirical cotidal charts. Based on the continuity of harmonic constants in space, we apply the harmonics on T/P tracks to fit those between T/P tracks so that the harmonics in the whole study areas can be estimated.

---

*Corresponding author address:* Xian-Qing Lv, Laboratory of Physical Oceanography, Ocean University of China, Qingdao 266100, China.  
E-mail: xqinglv@ouc.edu.cn

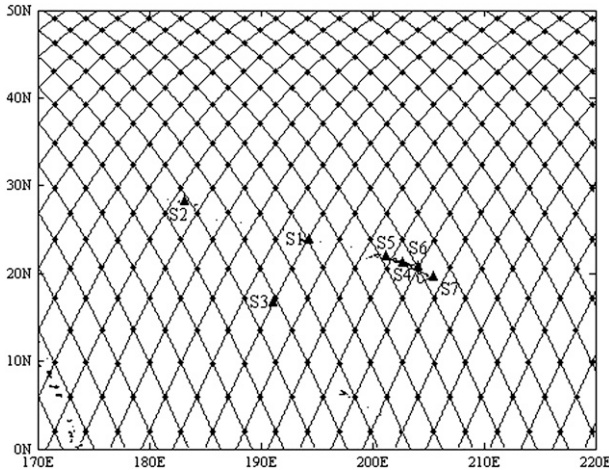


FIG. 1. Distributions of TOPEX/Poseidon ground tracks and tidal stations near Hawaii. The T/P ground tracks (lines), T/P crossover points (dots), islands (small dark areas), and (S1–S7) tidal stations (triangles) are shown.

The paper is organized as follows. Harmonic analysis of 10 yr of T/P along-track altimetry is performed to derive eight principal constituents near Hawaii, and the T/P solutions are evaluated through an intercomparison for crossover points and a comparison with the data of tidal stations in section 2. In section 3, harmonic constants of any point on T/P tracks are acquired by using suitable-order polynomials to fit T/P solutions along every track. In section 4, a new fitting method, which is characterized by applying the harmonics from T/P tracks to produce empirical cotidal charts, is developed and evaluated through comparison with the data from tidal stations, the results of the National Astronomical Observatory 99b (NAO.99b), TOPEX/Poseidon 7.2 (TPX07.2), and Finite Element Solutions 2004 (FES2004) models. The paper ends with conclusions in section 5.

## 2. Harmonics derived from T/P altimeter data

The T/P altimeter data from October 1992 to June 2002 (2 ~ 363 cycles), which we use in this paper, is provided by the National Aeronautics and Space Administration (NASA). First, we process the approximately 10 yr of T/P altimeter data to gain the time series of tidal elevations of each observation point on the tracks. Then, we make use of this information to perform harmonic analyses for deriving the harmonics. Considering that too few observation times may lower the reliability of harmonic analysis, we only select the points that have more than 300 T/P observations.

### a. Intercomparison of T/P-derived harmonics at crossover points

There are in total 339 crossover points on the 54 ground tracks (27 ascending and 27 descending ground

TABLE 1. RMS of amplitude difference and vector difference at 339 crossover points between harmonics derived from ascending and descending tracks for eight principal constituents. Respectively,  $\Delta H$  and  $\Delta$  represent amplitude difference and vector difference between them (cm).

|            | $M_2$ | $S_2$ | $N_2$ | $K_2$ | $K_1$ | $O_1$ | $P_1$ | $Q_1$ |
|------------|-------|-------|-------|-------|-------|-------|-------|-------|
| $\Delta H$ | 0.76  | 0.96  | 0.69  | 1.76  | 1.67  | 0.83  | 1.05  | 0.91  |
| $\Delta$   | 1.06  | 0.99  | 1.03  | 1.20  | 2.51  | 1.16  | 1.65  | 1.44  |

tracks) within the study area, which are indicated by red dots in Fig. 1. We carry out comparisons of harmonics at 339 crossover points for the eight principal constituents ( $M_2$ ,  $S_2$ ,  $N_2$ ,  $K_2$ ,  $K_1$ ,  $O_1$ ,  $P_1$ , and  $Q_1$ ). Because of the limited space, we only give the RMS of amplitude difference and vector difference for 339 crossover points in Table 1. The vector difference  $\Delta$  between the ascending and descending solutions (Fang et al. 2004) is defined by

$$\Delta = [(H_a \cos G_a - H_d \cos G_d)^2 + (H_a \sin G_a - H_d \sin G_d)^2]^{1/2}, \quad (1)$$

where the subscripts  $a$  and  $d$  represent ascending and descending solutions, respectively.

From Table 1, we can see that the RMS of the amplitude difference for eight principal constituents is less than 2 cm, and the maximum and minimum are 1.76 ( $K_2$  tide) and 0.69 ( $N_2$  tide) cm, respectively; the RMS of vector difference is about 2 cm, and the maximum and minimum are 2.51 ( $K_1$  tide) and 0.99 ( $S_2$  tide) cm, respectively. These small differences indicate that the T/P solutions we obtained above are reliable.

### b. Comparison between T/P-derived harmonics and the data of tidal stations

We download the sea level data of seven tidal stations (online at <http://www.soest.hawaii.edu/UHSLC/>), which are indicated by green triangles in Fig. 1, and we perform harmonic analyses for them. The amplitude difference and vectorial difference between the T/P solutions and the data from the tidal stations for eight principal constituents are listed in Tables 2 and 3.

From Tables 2 and 3, we can see that the RMS of the amplitude difference for the eight principal constituents is less than 2 cm, for example, the maximum and minimum are 1.73 ( $M_2$  tide) and 0.47 ( $N_2$  tide) cm, respectively; the RMS of the vector difference for eight principal constituents is less than 3; and the maximum and minimum are 2.95 ( $M_2$  tide) and 0.99 ( $N_2$  tide) cm, respectively. These comparisons validate the T/P solutions.

## 3. Acquisition of harmonics on T/P tracks

Cummins et al. (2001) separated the barotropic and internal tide by using an eighth-order polynomial to fit



TABLE 4. Comparisons of the mean value of the amplitude difference and phase-lag difference of the  $M_2$  tide between T/P solutions and harmonics derived by polynomial fitting for all the tracks.

| Order    | 3    | 4    | 5    | 6    | 7    | 8    | 9    | 10   | 11   | 12   | 13   | 14   | 15   |
|----------|------|------|------|------|------|------|------|------|------|------|------|------|------|
| $H$ (cm) | 0.72 | 0.61 | 0.55 | 0.70 | 0.52 | 0.51 | 0.50 | 0.49 | 0.49 | 0.49 | 0.64 | 0.49 | 0.56 |
| $G$ (°)  | 3.67 | 3.41 | 3.16 | 3.05 | 2.94 | 2.91 | 2.78 | 2.72 | 2.62 | 2.66 | 4.83 | 2.89 | 2.81 |

$$\begin{bmatrix} M_{1,1} & M_{1,2} & M_{1,3} & \cdots & M_{1,n+1} \\ M_{2,1} & M_{2,2} & M_{2,3} & \cdots & M_{2,n+1} \\ M_{3,1} & M_{3,2} & M_{3,3} & \cdots & M_{3,n+1} \\ \vdots & \cdots & \cdots & \cdots & \cdots \\ M_{n+1,1} & M_{n+1,2} & M_{n+1,3} & \cdots & M_{n+1,n+1} \end{bmatrix} \cdot \begin{bmatrix} a_0 \\ a_1 \\ a_2 \\ \cdots \\ a_n \end{bmatrix} = \begin{bmatrix} b_1 \\ b_2 \\ b_3 \\ \cdots \\ b_{n+1} \end{bmatrix}. \quad (6)$$

The values of  $a_0, a_1, a_2, \dots, a_n$  are obtained by solving the above linear Eq. (6), and substituting these parameters into Eq. (2) yields the values of the barotropic tide, that is,

$$\hat{f}(y) = a_0 + a_1 y + a_2 y^2 + \cdots + a_n y^n. \quad (7)$$

Similarly, we can also get

$$\hat{g}(y) = a_0 + a_1 y + a_2 y^2 + \cdots + a_n y^n, \quad (8)$$

by progressing the values of  $H \sin G$  for the  $M_2$  tide with the similar method.

According to the method above, we use 3rd–15th-order polynomials to fit the values of  $H \cos G$  and  $H \sin G$  for the  $M_2$  tide along every track, respectively. The mean values of the amplitude difference and phase-lag difference of the  $M_2$  tide between the T/P solutions and harmonics derived by polynomial fitting for all the tracks are given in Table 4.

From Table 4, we can see that using a higher order in polynomial fitting does not lead to a smaller difference. The mean value of the amplitude difference for all of the tracks by 10th-, 11th-, 12th-, and 14th-order polynomial fitting are all equal to 0.49 cm, which are much better than the other results. We can obviously see that the mean value of the phase-lag difference for all of the tracks by the 11th polynomial fitting is the smallest. Thus, we choose the 11th-order polynomial to fit the values of  $H \cos G$  and  $H \sin G$  for the  $M_2$  tide along every track, respectively. Then, the values of  $H \cos G$  and  $H \sin G$  for the  $M_2$  tide at any point on the tracks are acquired.

#### 4. Development of the fitting method

In this section, a new fitting method, which is characterized by the application the harmonics from T/P

tracks to produce an empirical cotidal chart, is developed. We select any point  $p$  in the study area. Based on the ratio of the distances between this point and its two nearest ascending (descending) tracks, a series of points on the descending (ascending) tracks that have the same ratio with this point between the two ascending (descending) tracks are obtained. By fitting the harmonics of these points with a suitable-order polynomial, the values of amplitude and phase lag of this point  $p$  are acquired. Here, we will describe this fitting method in detail.

##### a. Identify the four nearest tracks to point $p$

A series of quadrangles in the study area are surrounded by ascending and descending tracks as shown in Fig. 1. If we want to acquire the harmonic constants of point  $p$  in the study area, we should first know the quadrangle in which this point is located. Meanwhile, the four nearest tracks to this point are identified.

As shown in Fig. 2, the necessary and sufficient conditions for point  $p(x, y)$  located in the quadrangle  $p_1 p_2 p_3 p_4$  are

point  $p$  is below straight line  $p_1 p_4 \Leftrightarrow y < [(y_4 - y_1)/(x_4 - x_1)](x - x_1) + y_1$ , point  $p$  is above straight line  $p_2 p_3 \Leftrightarrow y > [(y_3 - y_2)/(x_3 - x_2)](x - x_3) + y_3$ , point  $p$  is above straight line  $p_1 p_2 \Leftrightarrow y > [(y_2 - y_1)/(x_2 - x_1)](x - x_2) + y_2$ , and point  $p$  is below straight line  $p_3 p_4 \Leftrightarrow y < [(y_4 - y_3)/(x_4 - x_3)](x - x_4) + y_4$ .

If the above four conditions are satisfied, point  $p$  is located in the quadrangle  $p_1 p_2 p_3 p_4$ . The four nearest tracks to point  $p$ , the ascending ( $i, i + 1$ ) and descending ( $j, j + 1$ ) tracks, are identified.

TABLE 5. Amplitude difference and vector difference between harmonics derived from tidal stations and those obtained by this fitting method for  $M_2$  tide (cm).

| Station | °N/°E        | $\Delta H$ | $\Delta$ |
|---------|--------------|------------|----------|
| S1      | 28.22/182.63 | 2.02       | 2.62     |
| S2      | 16.75/190.48 | 2.54       | 2.54     |
| S3      | 23.87/193.71 | 0.09       | 1.62     |
| S4      | 21.96/200.64 | 1.51       | 4.18     |
| S5      | 21.43/202.21 | 1.30       | 3.96     |
| S6      | 20.90/203.53 | 2.03       | 5.66     |
| S7      | 19.73/204.93 | 3.09       | 3.10     |
| RMS     |              | 2.01       | 3.60     |

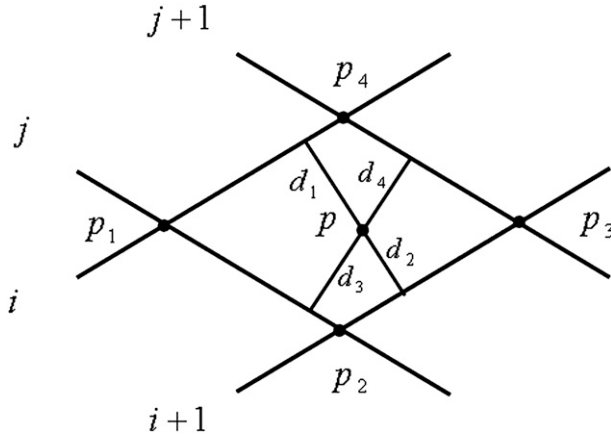


FIG. 2. Point  $p$  is located in the quadrangle  $p_1p_2p_3p_4$  that is surrounded by two adjacent ascending tracks  $(i, i + 1)$  and two adjacent descending tracks  $(j, j + 1)$ . Four vertices of the quadrangle are  $p_1(x_1, y_1)$ ,  $p_2(x_2, y_2)$ ,  $p_3(x_3, y_3)$ , and  $p_4(x_4, y_4)$ , respectively;  $d_1, d_2, d_3, d_4$  are the distances between the point  $p$  and four sides ( $p_1p_4, p_2p_3, p_1p_2, p_3p_4$ ), respectively.

*b. Calculate the distances between point  $p$  and its four nearest tracks*

According to the longitude and latitude of point  $p$  and four vertices of its quadrangle, the distances between the point and four sides are computed, which are the distances between this point and its four nearest tracks. Here, we calculate the distance between point  $p$  and side  $p_1p_2$  as an example.

First, calculate the side length of  $\Delta p p_1 p_4$  according to the distance formula of two points on the sphere

$$L = R \cdot \arccos[\sin\beta_1 \sin\beta_2 + \cos\beta_1 \cos\beta_2 \cos(\alpha_1 - \alpha_2)],$$

where  $R$  represents the radius of the earth,  $\alpha_1, \alpha_2$  is the longitude of two points, respectively, and  $\beta_1, \beta_2$  is the latitude of two points, respectively. The lengths of three sides of  $\Delta p p_1 p_4$  are computed, respectively.

Second, calculate the area of  $\Delta p p_1 p_4$  according to the area of a triangle

$$s = \sqrt{l(l - pp_1)(l - pp_4)(l - p_1p_4)}, \quad (9)$$

where  $l$  is half circumference of  $\Delta p p_1 p_4$  and the area of  $\Delta p p_1 p_4$  is counted.

Third, calculate the distance between point  $p$  and side  $p_1p_4$ ; the area formula of  $\Delta p p_1 p_4$  can be also expressed as

$$s = (d_1 \times p_1p_4)/2, \quad (10)$$

where  $d_1$  is the distance between point  $p$  and side  $p_1p_4$ . According to (9) and (10), the distance

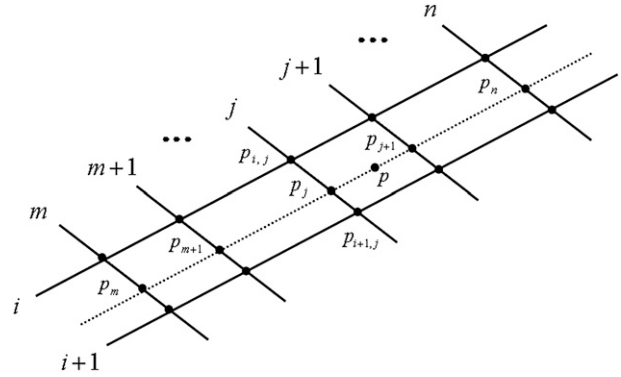


FIG. 3. Point  $p$  is located between two adjacent ascending tracks  $(i, i + 1)$ , and  $n - m + 1$  descending tracks  $(m, m + 1, \dots, j, j + 1, \dots, n)$  pass through the two ascending tracks. A series of points  $p_m, p_{m+1}, \dots, p_j, p_{j+1}, \dots, p_n$  that have the same ratio with point  $p$  between the two adjacent ascending tracks lie on the  $n + (m - 1)$  descending tracks, respectively.

$$d_1 = 2\sqrt{l(l - pp_1)(l - pp_4)(l - p_1p_4)/p_1p_4},$$

where  $l = (pp_1 + pp_4 + p_1p_4)/2$  is reckoned. Similarly, we can calculate the distances ( $d_2, d_3, d_4$ ) between point  $p$  and the other three sides ( $p_2p_3, p_1p_2, p_3p_4$ ). Then, the distances ( $d_1, d_2$ ) between point  $p$  and its two nearest ascending tracks  $(i, i + 1)$  and the distances ( $d_3, d_4$ ) between point  $p$  and its two nearest descending tracks  $(j, j + 1)$  are known (see Fig. 2).

*c. Fit the harmonic constants of point  $p$*

For point  $p$  in the study area, it may be located on the track or outside the track. If this point is on the track, the harmonic constants of this point are obtained according to the polynomials in the third part. Otherwise they are acquired by the fitting method described below:

Step 1: As shown in Fig. 3, according to the ratio of the distances between point  $p$  and its two nearest ascending tracks, a series of points ( $p_m, p_{m+1}, \dots, p_j, p_{j+1}, \dots, p_n$ ) on these  $n + (m - 1)$  descending tracks that have the same ratio with point  $p$  between two adjacent ascending tracks are acquired. For example, point  $p_j$  on the descending track  $(j)$  is obtained by  $\mathbf{op}_j = w_1 \times \mathbf{op}_{i,j} + w_2 \times \mathbf{op}_{i+1,j}$ , where  $o$  represents the origin of coordinate,  $w_1 = d_2/(d_1 + d_2)$ , and  $w_2 = d_1/(d_1 + d_2)$  are the weight values between point  $p$  and ascending tracks  $(i, i + 1)$ , respectively.

Step 2: Based on polynomials in the third part, the values of  $\hat{f}(y)$  and  $\hat{g}(y)$  of any point on the tracks are acquired, where  $\hat{f}(y) = H \cos G$  and  $\hat{g}(y) = H \sin G$ . Thus, the values of  $H_j \cos G_j$  and  $H_j \sin G_j$  ( $j = m, m + 1, \dots, n$ ) of the series of points ( $p_m, p_{m+1}, \dots, p_j, p_{j+1}, \dots, p_n$ ) can be derived.



TABLE 6. Amplitude difference and phase-lag difference between harmonics derived from models and those obtained by this fitting method for the  $M_2$  tide.

| Models  | Data points | $\Delta H$ (%) |       |       |       | $\Delta G$ (%) |      |      |      |
|---------|-------------|----------------|-------|-------|-------|----------------|------|------|------|
|         |             | RMS (°)        | <1 cm | <2 cm | <3 cm | RMS (°)        | <1°  | <3°  | <5°  |
| NAO99b  | 6077        | 1.99           | 31.9  | 57.6  | 89.2  | 2.44           | 50.1 | 82.9 | 94.1 |
| TPXO7.2 | 24 617      | 1.89           | 32.0  | 62.8  | 90.5  | 3.17           | 51.1 | 83.2 | 94.8 |
| FES2004 | 97 817      | 2.09           | 37.1  | 60.0  | 80.7  | 3.68           | 41.9 | 76.3 | 92.6 |

Step 3: We use 3rd–15th-order polynomials to fit the values of  $H_j \cos G_j$  and  $H_j \sin G_j$  ( $j = m, m + 1, \dots, n$ ) of these  $n - (m + 1)$  points, respectively, which is similar to the third step. Based on the minimum residual, we select the most suitable polynomials as follow:

$$\begin{aligned}\tilde{f}(y) &= a_0 + a_1 y + a_2 y^2 + \dots + a_l y^l \quad \text{and} \\ \tilde{g}(y) &= a_0 + a_1 y + a_2 y^2 + \dots + a_l y^l.\end{aligned}$$

According to the two polynomials, the values of  $\tilde{f}(y)$  and  $\tilde{g}(y)$  of point  $p$  are acquired, where  $\tilde{f}(y) = H \cos G$  and  $\tilde{g}(y) = H \sin G$ . Finally, the values of the amplitude  $H$  and phase lag  $G$  of point  $p$  are obtained by coordinate transformation.

Similarly, the values of the amplitude and phase lag of point  $p$  can be derived by fitting a series of points on the ascending tracks between its two nearest descending tracks.

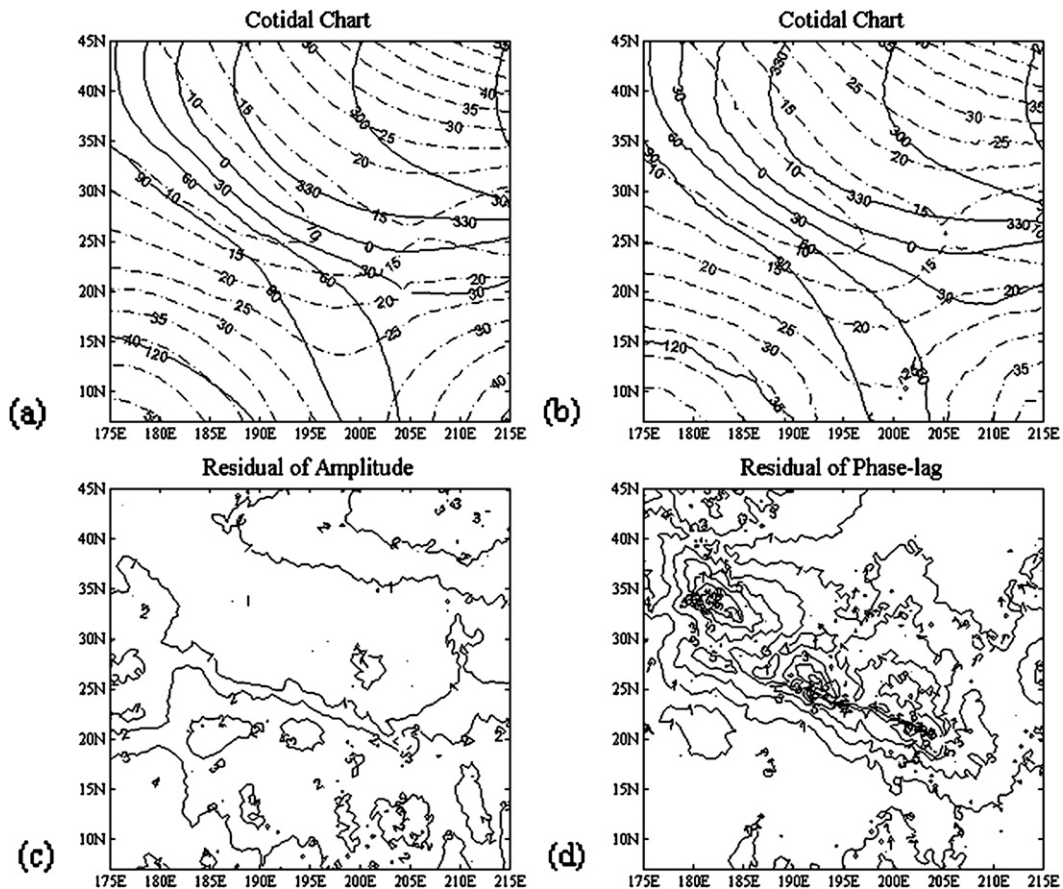


FIG. 4. Cotidal charts of the  $M_2$  tide near Hawaii obtained from (a) the NAO.99b model and (b) the fitting method, and comparisons of (c) amplitude and (d) phase lag between them, with a spatial resolution of  $0.5^\circ$ . Phase lag ( $^\circ$ ; solid line) and amplitude (cm; dashed line) are shown.

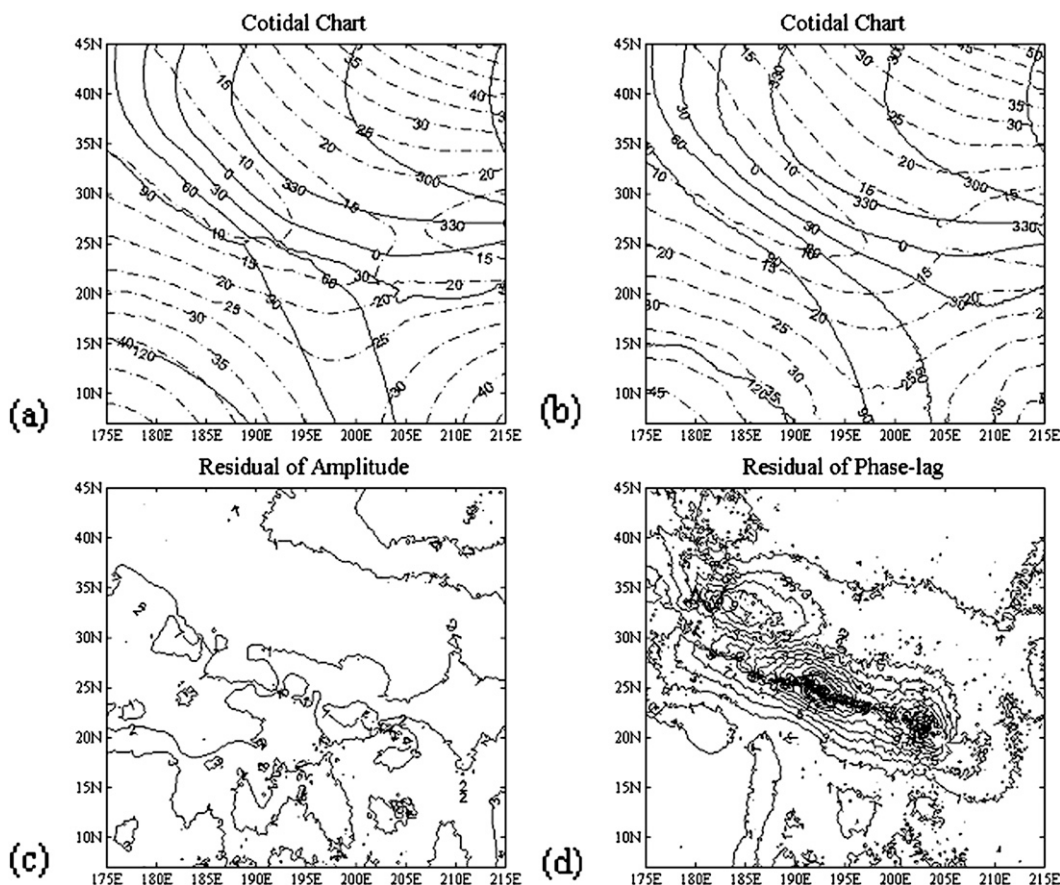


FIG. 5. As in Fig. 4, but for the TPXO7.2 model with (d) a spatial resolution of  $0.25^\circ$ .

In a word, the harmonic constants of point  $p$  can be acquired by fitting a series of points on the ascending tracks between its two nearest descending tracks or on the descending between its two nearest ascending tracks. However, which one is selected to get the values of amplitude and phase lag of point  $p$  depends on the number of fitting points. If the number of fitting points on the ascending tracks is more than that on the descending tracks, the harmonics of point  $p$  are obtained by fitting a series of points on the ascending tracks. Otherwise, the harmonics of point  $p$  are derived by fitting a series of points on the descending tracks.

#### d. Evaluation of the fitting method

The new fitting method cannot only be applied to any open sea, but also can be popularized to any tide. To evaluate this fitting method, we carry out comparisons of harmonic constants of the  $M_2$  tide derived by this fitting method with the data of tidal stations, the results of the NAO.99b, TPXO7.2, and FES2004 models.

#### 1) COMPARISON WITH THE DATA OF TIDAL STATION

We acquire the harmonic constants of the  $M_2$  tide at seven tidal stations (see Fig. 1) by this fitting method and carrying out a comparison with local harmonics. Table 5 gives the amplitude difference and the vectorial difference of the  $M_2$  tide between them. The last line is the RMS of the amplitude difference and vectorial difference of the  $M_2$  tide for seven tidal stations.

From Table 5, we can see that the RMS of the amplitude difference and vector difference of the  $M_2$  tide at seven tidal stations are 2.01 and 3.60 cm, respectively. The minimum of the amplitude difference and vector difference, which is shown at S3, are 0.09 cm and 1.62 cm, respectively. Fairly good agreement with the data of tidal stations validates the new fitting method.

#### 2) COMPARISON WITH MODELS

The NAO.99b model, which is a global model representing 16 constituents with a spatial resolution of  $0.5^\circ$ , is developed by assimilating tidal solutions from about

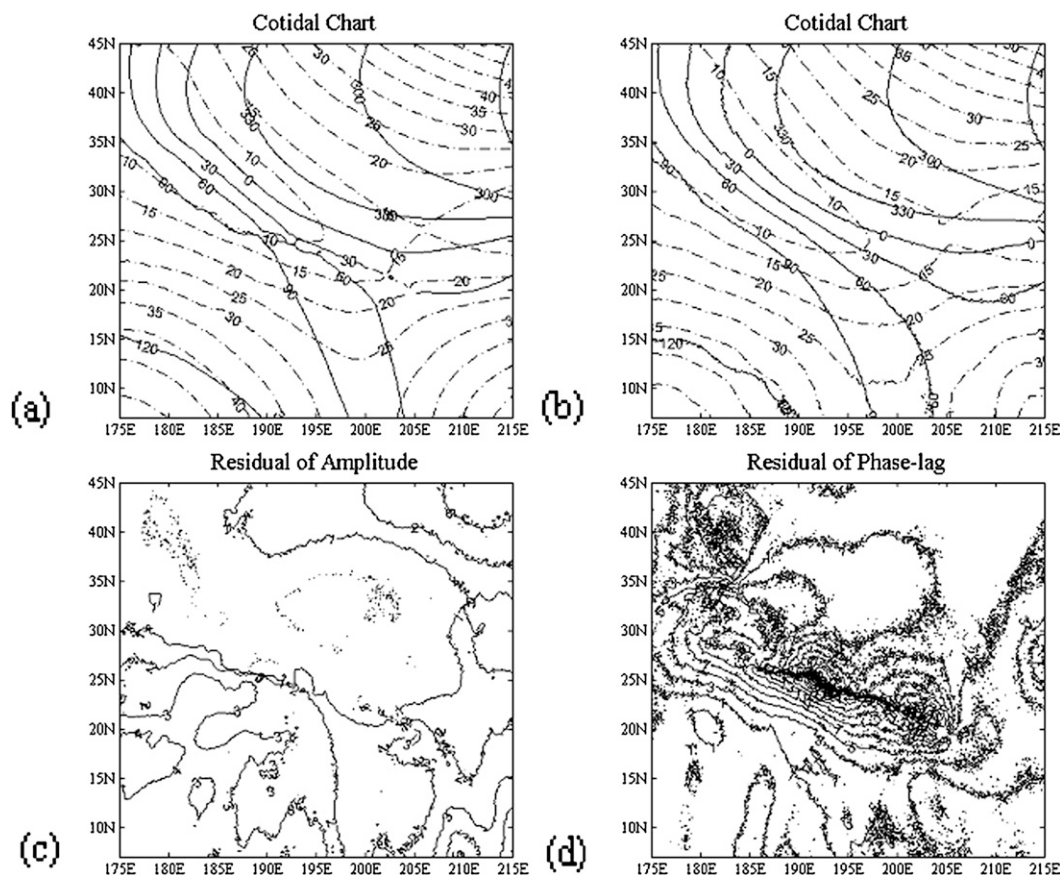


FIG. 6. As in Fig. 4, but for the FES2004 model with (d) a spatial resolution of  $0.125^\circ$ .

5 yr of T/P altimeter data into a barotropic hydrodynamic model. Matsumoto et al. (2000) examined the accuracy of the model using tide gauge data and a collinear residual reduction test, which showed a comparable agreement with 98 open-ocean tide gauge data as well as CSR4.0 and GOT99.2b.

The TPX07.2 model is a medium-resolution,  $1/4^\circ \times 1/4^\circ$  global model developed by G. Egbert and L. Erofeeva at Oregon State University (OSU). It best fits, in a least squares sense, the Laplace tidal equations and along-track-averaged data from T/P and *Jason-1* obtained with OSU Tidal Inversion Software (OTIS). The methods used to compute the model are described in detail by Egbert et al. (1994) and further by Egbert and Erofeeva (2002).

The FES2004 model, which is a global model representing 15 constituents with a spatial resolution of  $0.125^\circ$ , is the latest release in a series of finite-element solutions tidal atlases that produced by the French tidal group. Lyard et al. (2006) introduce the FES2004 tidal atlas and validate the model against in situ and satellite data.

Through the fitting method of this paper, we acquire the harmonics of the  $M_2$  tide at the same grid point with the three models above and conduct a detailed comparison with the results of the models, which is shown in Table 6. Additionally, the cotidal charts of the  $M_2$  tide derived from this fitting method and the models and the deviation charts of amplitude and phase lag between them are mapped in Figs. 4–6, respectively.

From Table 6, we can see that the RMS of the amplitude differences between our data and the results from the models are about 2 cm, and the amplitude differences at 60% of the grid points are smaller than 2 cm; the RMS of the phase-lag differences between them are about  $3^\circ$  and phase-lag differences at 80% of the points are smaller than  $3^\circ$ . From Figs. 4 to 6, the comparison of cotidal charts shows that the amplitude lines basically have the same trend; also, the agreement of the phase-lag lines is very good. There is a good agreement between the cotidal charts of the  $M_2$  tide obtained by the fitting method of this paper and those derived from the NAO.99b, TPX07.2, and FES2004 models. Thus, the new fitting method is believed to be reasonable.



## 5. Conclusions

In this paper, harmonic analysis of 10 yr of T/P along-track altimetry is performed to derive eight constituents' harmonic constants near Hawaii. The intercomparison between the T/P solutions of ascending and descending tracks at crossover points shows that the mean RMS of the amplitude variation  $\Delta H$  are between 0.69 and 1.76 cm, and the mean RMS of the vector differences  $\Delta$  range from 0.99 to 2.51 cm, which validate the precision of the T/P solutions in this study area. Based on these, the harmonics of any point on the T/P tracks are acquired by using suitable polynomials to fit the values of  $H \cos G$  and  $H \sin G$  along every track. Then, we introduce a new method to get harmonics between T/P tracks by fitting the values of  $H \cos G$  and  $H \sin G$  on T/P tracks so that the harmonics in the whole study areas can be obtained. To evaluate this fitting method, we carry out a series of comparisons of the  $M_2$  tide with the data of tidal stations, the results of NAO.99b, TPXO7.2, and FES2004 models. The results show that the RMS of the amplitude differences between our data and the results from models are about 2 cm; the RMS of the phase-lag differences between them are about  $3^\circ$ . In addition, the comparison of cotidal charts shows that the amplitude lines basically have the same trend; the agreement of the phase-lag lines is also very good. Thus, the fitting method is believed to be reasonable and the highly accurate cotidal charts could be directly acquired from T/P altimetry data by this fitting method.

The new fitting method can be applied to any tide in the open sea. Compared with other existing methods and models, the advantage of this method in our paper is that the workload is greatly reduced, hence, leading to the speeding up of the calculations significantly. It not only adds to the ways to obtain cotidal charts, but also popularizes the application of altimeter data.

**Acknowledgments.** We deeply thank the reviewers and editor for their constructive suggestions on the earlier version of the manuscript. Thanks are extended to the Aviso Team for providing us the result of the FES2004

model. This work was supported by the State Ministry of Science and Technology of China (2007AA09Z118 and 2008AA09A402), the National Natural Science Foundation of China under Contract 41076006, and the Ministry of Education's 111 Project (B07036).

## REFERENCES

- Cummins, P. F., J. Y. Cherniawski, and M. G. Foreman, 2001: North Pacific internal tides from the Aleutian Ridge: Altimeter observations and modeling. *J. Mar. Res.*, **59**, 167–191.
- Dushaw, B. D., 2002: Mapping low-mode internal tides near Hawaii using TOPEX/Poseidon altimeter data. *Geophys. Res. Lett.*, **29**, 1250, doi:10.1029/2001GL013944.
- Egbert, G. D., and S. Y. Erofeeva, 2002: Efficient inverse modeling of barotropic ocean tides. *J. Atmos. Oceanic Technol.*, **19**, 183–204.
- , A. F. Bennett, and M. G. G. Foreman, 1994: TOPEX/POSEIDON tides estimated using a global inverse model. *J. Geophys. Res.*, **99**, 24 821–24 852.
- Fang, G. H., 1986: Tide and tidal current charts for the marginal seas adjacent to China. *Chin. J. Oceanol. Limnol.*, **4**, 1–16.
- , Y. G. Wang, Z. X. Wei, B. H. Choi, X. Y. Wang, and J. Wang, 2004: Empirical cotidal charts of the Bohai, Yellow, and East China Seas from 10 years of TOPEX/Poseidon altimetry. *J. Geophys. Res.*, **109**, C11006, doi:10.1029/2004JC002484.
- Lyard, F., F. Lefevre, T. Letellier, and O. Francis, 2006: Modelling the global ocean tides: Modern insights from FES2004. *Ocean Dyn.*, **56**, 394–415.
- Matsumoto, K., T. Takanezawa, and M. Ooe, 2000: Ocean tide models developed by assimilating TOPEX/POSEIDON altimeter data into hydrodynamical model: A global model and a regional model around Japan. *J. Oceanogr.*, **56**, 567–581.
- Mazzega, P., and M. Berge, 1994: Ocean tides in the Asian semi-enclosed seas from TOPEX/POSEIDON. *J. Geophys. Res.*, **99**, 24 867–24 881.
- Nishida, H., 1980: Improved tidal charts for the western part of the North Pacific Ocean. *Rep. Hydrogr. Res.*, **15**, 55–70.
- Ogura, S., 1933: The tides in the seas adjacent to Japan. Imperial Japanese Navy, Bulletin of the Hydrographic Department No. 7, 189 pp.
- Teague, W. J., P. Pistek, G. A. Jacobs, and H. T. Perkins, 2000: Evaluation of tides from TOPEX/Poseidon in the Bohai and Yellow Seas. *J. Atmos. Oceanic Technol.*, **17**, 679–687.
- Yanagi, T., A. Morimoto, and K. Ichikawa, 1997: Co-tidal and co-range charts for the East China Sea and the Yellow Sea derived from satellite altimetric data. *J. Oceanogr.*, **53**, 303–309.